DYNAMIC PROPERTIES AND MEMBRANE ACTIVITY OF ION SPECIFIC ANTIBIOTICS

E. Grell and Th. Funck

Max-Planck-Institut für biophysikalische Chemie, Göttingen, Germany

Conformational rearrangements of membrane-active peptide and depsipeptide antibiotics such as enniatin B, valinomycin, and valine-gramicidin A have been studied as a function of solvent polarity employing ultrasonic absorption methods. The results provide information about the number of occupied conformational states and their respective rates of interconversion. The interpretation of the results from kinetic measurements was confirmed by spectroscopic studies.

The remarkable differences in the stabilities of the various cation complexes of depsipeptide antibiotics bound to lecithin vesicles as well as in homogeneous solution were related to different conformations of the ligands in these complexes as characterized by spectroscopic techniques. Kinetic studies by relaxation methods led to the elucidation of the mechanism of complex formation. Complexation of cations follows a multistep reaction. For valinomycin the rate-limiting step of cation complexation is a ligand conformational change which occurs during the stepwise substitution of solvent molecules from the cation.

INTRODUCTION

Membrane-active antibiotics such as the cyclodepsipeptides enniatin B (1, 2) and valinomycin (3, 4) (Fig. 1) as well as the linear peptide valine-gramicidin A (5) (Fig. 1) induce a specific transport of alkali ions through biological membranes (6, 7) and model membrane systems (8–10). Many essential functions of biological membranes such as the excitation of the nerve membrane are coupled to a fast and specific exchange of Na^+ and K^+ ions. Therefore an investigation of the molecular mechanisms involved in such antibiotic-mediated transport processes is of interest.

The cyclodepsipeptide antibiotics act as cation carriers in membranes (9–11) (Fig. 2). The transport of cations can be characterized by complex formation between the membrane-bound antibiotic in a suitable conformation and the cations at the membrane surface. The antibiotic can undergo a conformational rearrangement subsequent to complex formation resulting in a lipid soluble cation complex. Complexation is followed by a diffusion of the antibiotic cation complex across the membrane where the cation is released. The carrier action is completed by a back diffusion of the uncomplexed antibiotic mole-

List of Abbreviations: CD, Circular Dichroism; UV, Ultraviolet; NMR, Nuclear Magnetic Resonance; IR, Infrared; TMS, Tetramethylsilane; Val, V, Valinomycin; E., Enniatin: B. G, Gramicidin A; Hylv, α-Hydroxy isovaleric acid; Lac, Lactic acid.

Journal of Supramolecular Structure

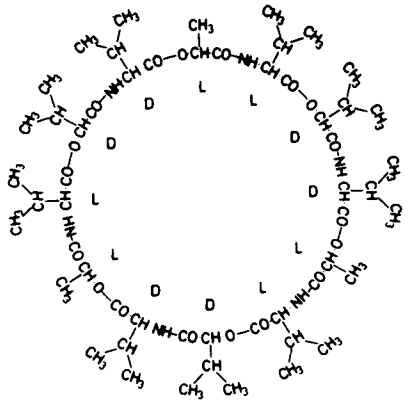

Valinomycin

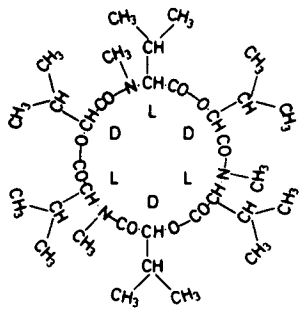

Enniatin B

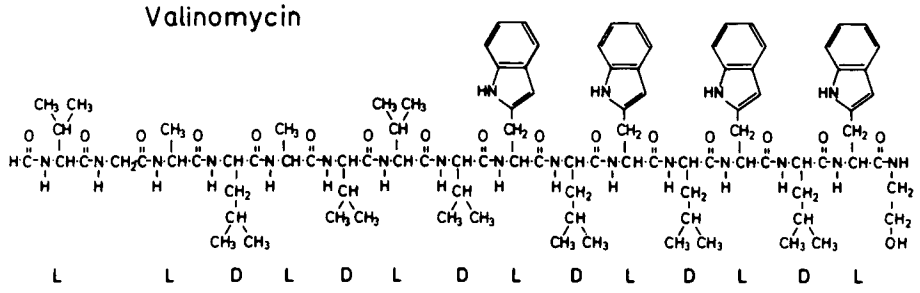

Gramicidin A

Fig. 1. Structure of valinomycin, enniatin B, and valine-gramicidin A.

cule. The rate constants for both diffusion steps are 2×10^4 sec^{-1} for valinomycin and its potassium complex (12). It is evident that the rates of these diffusion processes are limited by the fluidity properties of the membrane. Indeed, it has been demonstrated that the carrier action of valinomycin nearly disappears below the temperature of the crystalline–liquid crystalline phase transition (11).

On the other hand, the membrane-bound gramicidin A can act as a conductance channel for cations (13–16). It has been suggested that the channel 1 may conist of two antibiotic molecules which are present in a helical conformation (13–16) (Fig. 2). The life time of the conducting state of the dimer is sensitive to the membrane thickness and ranges from about 0.05 sec to greater than one minute (13, 16). The cation may be weakly coordinated by the gramicidin in its conducting state at the membrane surface. Upon this weak complex formation a diffusion of the cation through the pore can occur. During this diffusion step some slight conformational rearrangements of the antibiotic molecules might be expected. This is indicated schematically in Fig. 2. The rate constants for the diffusion of the cations through the gramicidin channel are at least 10^7 sec^{-1}. The time required for the transport of a single cation (<0.1 μsec) is consistent with that observed for cation transport in biological membrane systems. Therefore the mechanism of cation transport via a conducting channel can be expected to be more relevant toward biological membrane systems than the carrier mechanism. In addition the cation transport through a channel is almost insensitive to the fluidity of the membrane (11), thus strongly

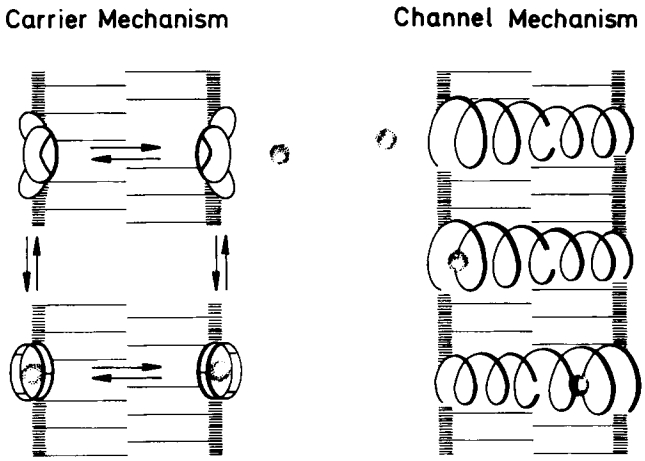

Fig. 2. Schematic diagram of the mechanisms involved in cation transport through membranes mediated by antibiotics.

supporting the classification of these antibiotics with respect to their ability to facilitate the transport of cations through membranes.

The outstanding ability of the membrane-bound antibiotics, which act as cation carriers, to differentiate between various alkali ions could also be observed in nonaqueous solvents in the absence of any membrane component (17–19) and was related to specific complex formation with the cations. Therefore these antibiotics have to be considered as relevant model systems for specific recognition of, or binding sites for, alkali ions in biological membrane systems. In contrast to the results obtained for the carrier molecule valinomycin, the cation selectivity of gramicidin A channels is rather poor.

EXPERIMENTAL METHODS

Circular dichroism experiments were performed on a Roussel–Jouan Dichrographe (Modèle CD 185). ([Θ] : molar ellipiticity).

High resolution ^{1}H–NMR spectra were obtained using a 100MHz Varian HA–100 instrument. Signal shifts (δ) are given in p.p.m. relative to the reference signal of TMS. The sample temperatures were about 30°C during the measurements.

The natural abundance ^{13}C–NMR spectra were recorded at 25.2 MHz on a Varian XL–100 spectrometer in the Fourier-transform mode with proton noise decoupling. The spectrometer was field/frequency locked using the deuterium in the corresponding deuterated solvent. For reference purposes, the solutions contained small amounts of TMS and CS_2. All chemical shifts (δ) are given in p.p.m. relative to the TMS internal reference standard. The sample temperatures were about 45°C during the measurements.

IR spectra were obtained using a Perkin–Elmer 521 spectrometer and cells (pathlengths 0.1 and 0.2 mm) with NaCl windows. The solutions were transferred to the cells under a dry N_2 atmosphere. In order to exclude the possible influence of NaCl dissolved from the window material the spectra of the uncomplexed valinomycin were also investigated in cells made with Irtran-5 windows. No differences could be observed. The wave numbers

were calibrated with a polystyrene foil.

Ultrasonic absorption was measured by a resonator method specially developed for kinetic studies in chemical systems with relaxation times shorter than 1 μsec. The measurements were carried out in collaboration with Dr. F. Eggers (17, 18, 22). The excess absorption of the system is expressed as $\alpha\lambda$ (ultrasonic excess absorption per wavelength) in the frequency range of approximately 0.5 to 35 MHz. It is determined from the difference in quality values (Q-factor) of a cylindrical resonator system consisting of a 1 ml sample compartment between two quartz transducers filled first with the sample solution and subsequently with a suitable reference liquid. Above 20 MHz a special pulse technique has been developed which also requires 1 ml of solution. Sample cells for both methods were made from inert materials such as stainless steel and teflon. The details of these techniques are discussed elsewhere (18–20).

The ultrasonic absorption per wavelength $\alpha\lambda$ due to the chemical system can be described as the sum of the absorption terms of the individual relaxation processes and the residual absorption (19):

$$\alpha\lambda = \sum_i A_i \frac{\omega\tau_i}{1 + (\omega\tau_i)^2} + B\omega \qquad (1)$$

where τ_i and A_i are the relaxation times and amplitude factors respectively of the individual processes involved; ω, equal to $2\pi f$, is the angular frequency and B the amplitude of the background absorption. The amplitude A of an absorption process depends on the relative population of the corresponding equilibrium states as well as on the difference in reaction volume and enthalpy of these states. The measured ultrasonic absorption spectrum is plotted as log ($\alpha\lambda$) as a function of log f. In the case of a single relaxation process one characteristic absorption curve is obtained exhibiting a maximum absorption at $f = 1/2\pi\tau$. If the experimental data must be considered as a superposition of several absorption curves due to various relaxation processes, then the sound absorption spectrum must be resolved into its individual components by curve fitting. The number of single absorption curves i is equal to the minimum number of reaction steps. Furthermore, in the case of unimolecular rearrangements it can be concluded that at least i + 1 equilibrium states are polulated (excluding certain cyclic reaction schemes).

A high-intensity UV light source, specially selected photomultipliers, and inert gas flushing were used to carry out relaxation measurements by the temperature-jump technique in the UV range (195–250 mμ) even under conditions of considerable solvent absorption. The details of this technique are described elsewhere (17, 19).

DISCUSSION

Conformational Flexibility of Ion Specific Antibiotics

The rates of cation transport through membranes mediated by a carrier or a conductance channel are high. Therefore the conformational adaptation of the antibiotics to cations of varying size as well as to media of different polarities as during the diffusion of the uncomplexed antibiotic through the membrane, must occur rapidly. We have undertaken kinetic investigations employing ultrasonic absorption techniques in order to obtain some information about the dynamics of conformational rearrangements of enniatin B,

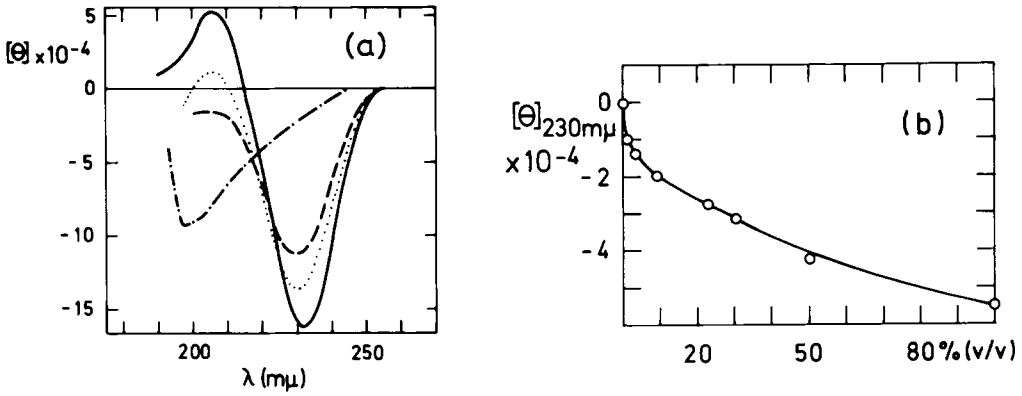

Fig. 3. (a) Circular dichroism of enniatin B in n-hexane (—); 30% ethanol in n-hexane (v/v) (. . . . .); ethanol (– – –); 38% water in ethanol (v/v) (–·–·). (T = 25°C). (b) Plot of the circular dichroism of enniatin B at 230 mμ against solvent composition [expressed as % ethanol in n-hexane (v/v)] in the system n-hexane/ethanol. (T = 25°C)

valinomycin, and valine-gramicidin as a function of a solvent polarity (17, 18, 22).

Enniatin B. The different spectroscopic properties of enniatin B observed in various solvent systems indicate that the antibiotic can exist in several conformational states (21, 22). In a nonpolar solvent such as n-hexane an intense negative Cotton effect due to the n-π^* transitions is found at 232 mμ (Fig. 3a). The intensity of this Cotton effect is reduced with increasing ethanol content in n-hexane indicating that a conformational transition occurs. The dependence of the molar ellipticity at 230 mμ as a function of the ethanol content in n-hexane is shown in Fig. 3b. From this dependence it is concluded that at least one conformational equilibrium between two different conformational states is involved. The relative populations of the two conformational states are about equal in n-hexane containing 25% of ethanol. A different type of CD spectrum is found in solvent systems of considerably higher polarity than ethanol, e.g., 38% water in ethanol (Fig. 3a). This indicates that enniatin B can undergo further conformational rearrangements.

Additional details of these processes can be concluded from the ^{1}H–NMR spectra of enniatin B in the same solvents. The dependence of chemical shifts of αCH protons of the amino acid ($\delta^{L-V}_{\alpha CH}$) and α-hydroxy acid ($\delta^{D-H}_{\alpha CH}$) residues on solvent composition are shown in Fig. 4. In the system d_{12}-cyclohexane/d_6-ethanol the measured dependence for the chemical shift of the αCH proton of the α-hydroxy acid residues is consistent with analogous experiments employing circular dichroism (Fig. 3b) and UV absorption spectrometry (18). This clearly indicates that the same conformational rearrangement can be observed employing any of these techniques.

The values of the coupling constants in the αCH–βCH fragments of enniatin B are nearly independent of the medium polarity, thus indicating that the trans orientation of protons in this structural element predominates in all conformational states present. The chemical shift of an αCH proton in an amino acid or hydroxy acid depends on the orientation of the neighboring carbonyl group relative to its own orientation in the molecule. This is due to differences in the magnetic anisotropy effect of the carbonyl group on the screening constant of the αCH proton. Therefore reorientations of ester and amide carbonyl

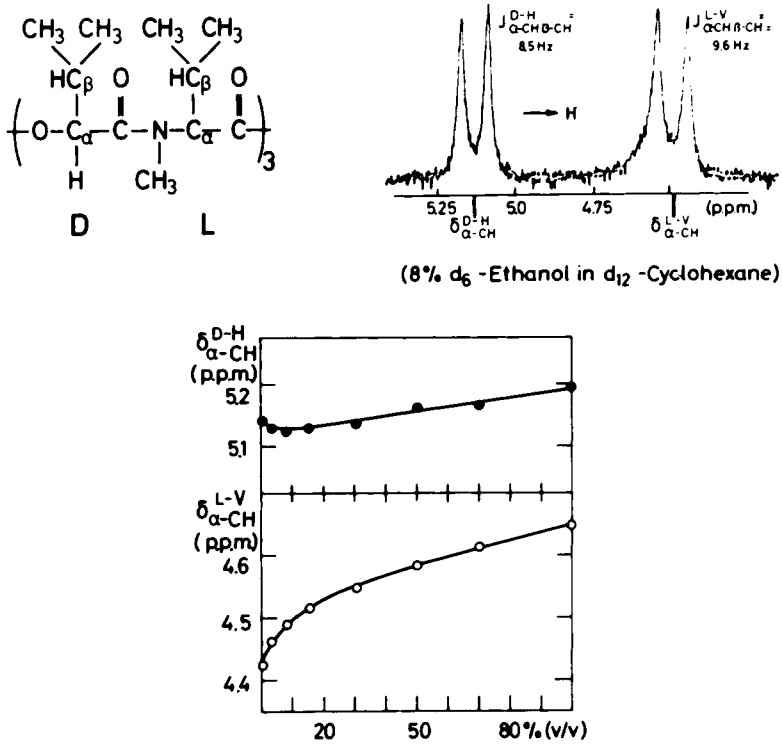

Fig. 4. Top: ^{1}H–NMR spectrum of αCH protons of enniatin B in 8% d_6-ethanol in d_{12}-cyclohexane (v/v) at 100 MHz. Bottom: The dependence of chemical shifts (δ) on solvent composition [expressed as % d_5-ethanol in d_{12}-cyclohexane (v/v)] in the system d_{12}-cyclohexane/d_5-ethanol.

groups in a cyclic molecule such as enniatin B should influence the chemical shift of the neighboring αCH protons. In the solvent system d_{12}-cyclohexane/d_6-ethanol only the chemical shift of the αCH proton of the N-methylvaline residue is markedly sensitive to the composition of the solvent, probably indicating a preferential reorientation of the neighboring ester carbonyl groups induced by a specific interaction (e.g., hydrogen bonds) with ethanol. On the other hand, in the more polar solvent systems additional changes in the ^{1}H–NMR spectrum of enniatin B were found (22). For an interpretation of these results on the basis of conformational rearrangements one must consider that in general NMR parameters can only be related to an averaged conformation rather than to individual conformational states.

Ultrasonic absorption measurements have been carried out in order to acquire some information about the dynamic aspects as well as to test the above conclusions with respect to the number of occupied conformational states deduced from the results of the equilibrium measurements.

In the case of enniatin B the sound absorption spectrum varies with the composition of the solvent in the system n-hexane/ethanol, as shown in Fig. 5. In pure n-hexane the ultrasonic absorption pattern can be described by a single absorption curve with a maximum amplitude around 100 MHz. It is therefore concluded that even in this nonpolar solvent there is at least one rather fast conformational transition between two major conformational states (cf. Table I) with a relaxation time of about 10^{-9} sec. Upon the addi-

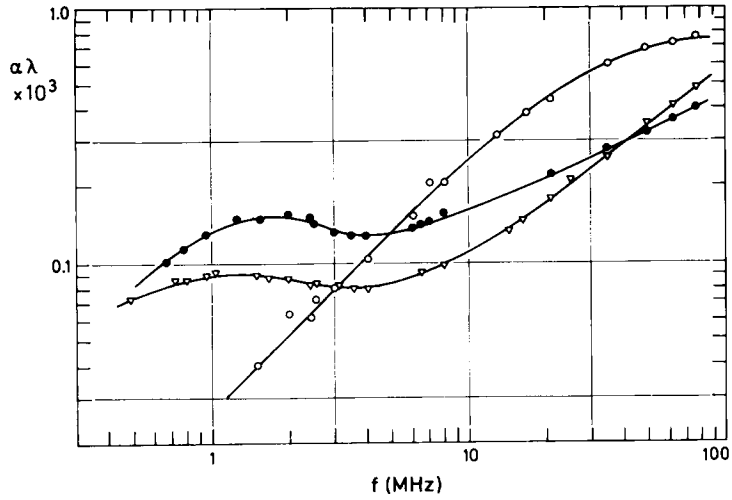

Fig. 5. Conformational transitions of enniatin B (5.2×10^{-2} M) in the solvent system n-hexane/ethanol. Frequency dependence of the ultrasonic excess absorption ($\alpha\lambda$) in n-hexane (○); 31% ethanol in n-hexane (v/v) (●); ethanol (△). (T = 25°C)

tion of ethanol the ultrasonic absorption was decreased in the frequency range of this relaxation and is furthermore characterized by a shift to higher frequencies. On the other hand, at lower frequencies (around 1.5 MHz) the ultrasonic absorption is increased as long as the ethanol content does not exceed 25%. An additional relaxation process can therefore be detected which was not observable in pure n-hexane. The relaxation time of the corresponding process in n-hexane containing 30% ethanol is 9×10^{-8} sec. The measured relaxation times are independent of the enniatin B concentration as expected for a unimolecular reaction. We can therefore conclude that upon the addition of ethanol at least three significantly populated conformational states are present (Table I). For an interpretation of this data one has to consider that more than one relaxation process could contribute to a single ultrasonic absorption curve under circumstances where the corresponding relaxation times would be very similar. On the other hand, conformational transitions between states which are characterized by only small differences in both reaction volume and enthalpy could not be detected employing this technique.

In Fig. 6 the dependence of the ultrasonic absorption at 1.7 MHz and 49 MHz is shown as a function of the solvent composition in the system n-hexane/ethanol. The dependence observed at 1.7 MHz exhibits a maximum for 25% ethanol in n-hexane. Making reasonable assumptions, this suggests that the equilibrium constant for the conformational states involved in the low frequency process is 1 under these experimental conditions. The sound absorption at 49 MHz is characterized by a different dependence on solvent composition. Such a dependence would be expected if the population of the conformational states involved in the 100 MHz process gradually decreases in favor of a third conformational state upon the addition of ethanol. The dependence of spectroscopic properties (circular dichroism, absorption, and ^{1}H–NMR spectrum (Fig. 3b, 4) (22) on solvent composition is only consistent with the amplitude dependence of the 1.7 MHz relaxation. This indicates that the differences in the spectroscopic properties mainly reflect changes in the conformational states which are involved in the slower relaxation process. A straight-

Table I. Conformational Transitions of Valinomycin and Enniation B in Different Solvents: Minimal Equilibrium Systems and Relaxation Times as Revealed by Ultrasonic Absorption Measurements.

Enniatin B	
n-Hexane	$\cdots \rightleftarrows E_1 \overset{\tau_1}{\rightleftarrows} E_2$ $\tau_1 \quad 2 \times 10^{-9}$ sec
n-Hexane/ethanol 5:1 (v/v)	$\cdots \rightleftarrows E_1 \overset{\tau_1}{\rightleftarrows} E_2 \overset{\tau_2}{\rightleftarrows} E_3$ $\tau_1 \quad 10^{-9}$ sec; $\tau_2 \quad 9 \times 10^{-8}$ sec
Methanol	$\cdots \rightleftarrows E_1 \overset{\tau_1}{\rightleftarrows} E_2 \overset{\tau_2}{\rightleftarrows} E_3$ $\tau_1 \quad 10^{-8}$ sec; $\tau_2 \quad 10^{-7}$ sec
Valinomycin	
n-Hexane	$\cdots \rightleftarrows V_1 \overset{\tau_1}{\rightleftarrows} V_2 \overset{\tau_2}{\rightleftarrows} V_3$ $\tau_1 \quad 2 \times 10^{-9}$ sec; $\tau_2 \; 2 \times 10^{-8}$ sec
n-Hexane/ethanol 1:1 v/v	$\cdots \rightleftarrows V_1 \overset{\tau_1}{\rightleftarrows} V_2 \overset{\tau_2}{\rightleftarrows} V_3 \overset{\tau_3}{\rightleftarrows} V_4$ $\tau_1 \quad 3 \times 10^{-9}$ sec; $\tau_2 \; 10^{-8}$ sec; $\tau_3 \; 10^{-7}$ sec
Methanol	$\cdots V_{n-1} \overset{\tau_n}{\rightleftarrows} V_n \cdots$ Spectrum of relaxation times τ_n

forward interpretation of the amplitude data as well as of the relaxation times is not possible without the availability of additional equilibrium parameters.

Nevertheless, some plausible estimates based on the following kinetic reaction scheme, which is the simplest that is consistent with the experimental results, can be obtained:

$$E_1 \underset{k_{21}}{\overset{k_{12}}{\rightleftarrows}} E_2 \underset{k_{32}}{\overset{k_{23}}{\rightleftarrows}} E_3$$

The corresponding equilibrium constants are

$$K_{12} = \frac{k_{21}}{k_{12}} \qquad (2) \qquad K_{23} = \frac{k_{32}}{k_{23}} \qquad (3)$$

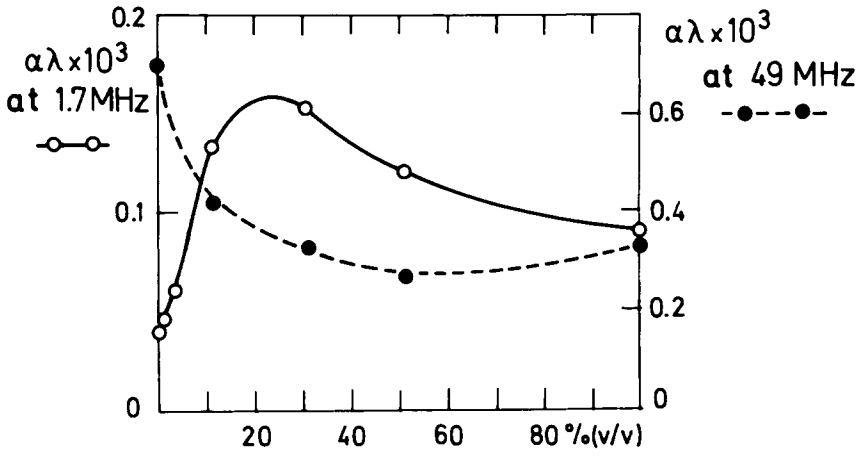

Fig. 6. Plot of ultransonic excess absorption of enniatin B (5.2×10^{-2} M) at 1.7 MHz (○) and 49 MHz (●) against solvent composition [expressed as % ethanol in n-hexane (v/v)] in the system n-hexane/ethanol. (T = 25°C)

If the step on the left-hand side of the above reaction scheme proceeds much faster than the right one, the two inverse relations times are given by

$$1/\tau_1 = k_{12} + k_{21} \tag{4}$$

$$1/\tau_2 = \frac{k_{23}}{1 + K_{12}} + k_{32} = k_{23}\left(K_{23} + \frac{1}{1 + K_{12}}\right) \tag{5}$$

τ_1 is assigned to the 100 MHz and τ_2 to the 1.7 MHz process. In the system 25% ethanol in n-hexane, a value of K_{23} of ~ 1 has been obtained from the amplitude dependence (Fig. 6). Under these experimentals conditions, therefore, k_{23} is equal to k_{32} and

$$1/\tau_1 = k_{12} + k_{21} = 10^9 \text{ sec}^{-1} \tag{6}$$

$$1/\tau_2 = k_{23}\left(1 + \frac{1}{1 + K_{12}}\right) = 1.1 \times 10^7 \text{ sec}^{-1} \tag{7}$$

Assuming certain values for K_{12} and substituting into eq. (7) it follows that

$$K_{12} \gg 1 \qquad 1/\tau_2 \approx k_{23} \tag{8}$$

$$K_{12} = 1 \qquad 1/\tau_2 = 1.5\, k_{23} \tag{9}$$

$$K_{12} \ll 1 \qquad 1/\tau_2 \approx 2\, k_{23} \tag{10}$$

It is evident that only the order of magnitude of k_{23} and k_{32} can be determined if K_{12} is not known. Nevertheless, it might be expected that the fast step can only be observed by ultrasonic absorption when K_{12} is of the order of 1. According to these plausible assumptions the rate constants k_{12} and k_{21} are of the order of 5×10^8 sec $^{-1}$ whereas k_{23} and k_{32} are of the order of 7×10^6 sec^{-1}.

These rate constants characterize the dynamic properties of the conformational re-

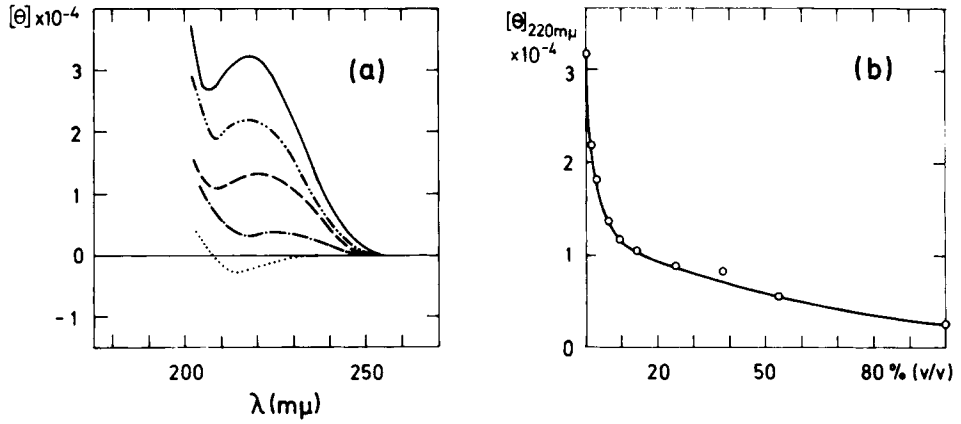

Fig. 7. (a) Circular dichroism of valinomycin in n-hexane (—), 1% ethanol in n-hexane (v/v) (– ·· – ··); 6% ethanol in n-hexane (v/v) (– – –); ethanol (– · – ·); trifluoroethanol (· · · · · ·). (b) Plot of the circular dichroism of valinomycin at 220 mμ against solvent composition [expressed as % ethanol in n-hexane (v/v)] in the system n-hexane/ethanol. (T = 25°C).

arrangements which are to a certain extent induced by specific solvent effects. The values of the rate constants are however too low for the direct recombination process to be due to the antibiotic and polar solvent molecules. On the other hand the faster relaxation process could be assigned to a rotation of the isopropyl side chains of the amino acid and hydroxy acid residues though such a process cannot be accompanied by a large volume change. However this interpretation is not expected to be a probable one since, according to the ^{1}H–NMR results, the preferential orientation of the side chains does not depend on the solvent composition. Thus, the amplitude of such a process should be independent of the ethanol content which is not consistent with the experimental results (Fig. 6). Since no intramolecular hydrogen bonds are possible within the enniatin B molecule it is concluded that the conformational changes in this solvent system are mainly due to a rearrangement of the ester carbonyl groups. This molecular interpretation is consistent with the results from ^{1}H–NMR studies. The dynamic properties of these rearrangement processes can be of significance during the coordination of a cation.

Valinomycin. Conformational rearrangements have also been suggested for valinomycin according to the spectral changes in solvents of varying polarity by employing spectroscopic techniques (21, 22).

The CD spectrum of valinomycin in nonpolar solvents such as n-hexane is mainly characterized by a positive Cotton effect at 218 mμ (Fig. 7a) which is sensitive to changes of solvent polarity. Upon addition of ethanol, this Cotton effect diminishes, while in trifluoroethanol it changes to a weak negative Cotton effect (Fig. 7a). The dependence of molar ellipticity at 220 mμ on solvent composition for the system n-hexane/ethanol is shown in Fig. 7b and indicates shifts in conformational equilibria. The dependence can be characterized by a two-step transition. The first is observed between pure n-hexane and around 30% ethanol in n-hexane, whereas the second occurs between the 30%

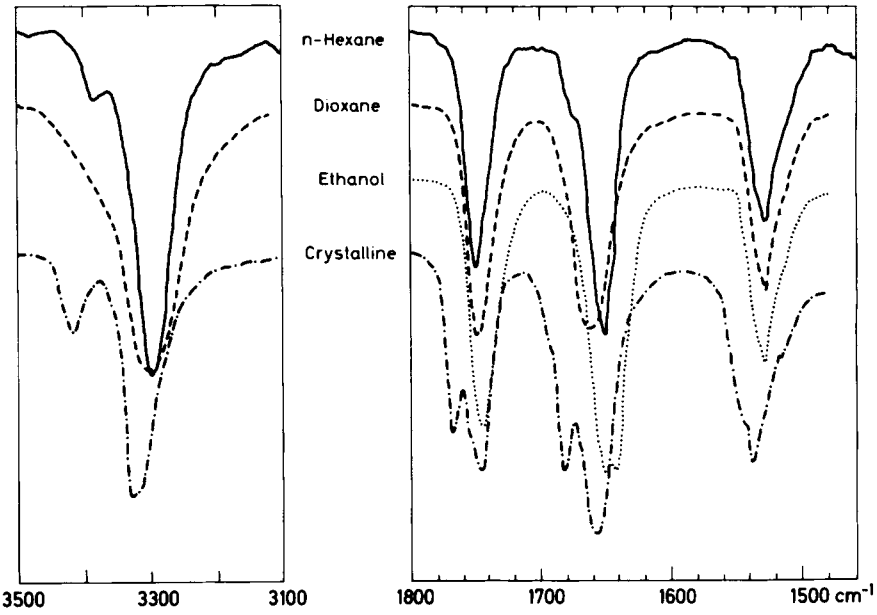

Fig. 8. Main bands of the IR absorption spectra of valinomycin in n-hexane (—); dioxane (– – –); ethanol (· · · · · ·). The spectrum of crystalline valinomycin (– · – ·) was obtained in the presence of Voltalef.

ethanol in n-hexane and pure ethanol. These results suggest a contribution of at least two conformational equilibria in the solvent system n-hexane/ethanol.

Remarkable differences are also found in the IR spectra of valinomycin in various solvents (Fig. 8). The spectrum observed in n-hexane is characterized by a much narrower ester and amide I band at 1750 cm^{-1} and 1651 cm^{-1}, respectively, compared to the absorp in ethanol (Fig. 8) or methanol (Fig. 18). In addition, the amide I band exhibits a pronounced inflection at 1675 cm^{-1} in n-hexane. The NH stretching frequencies could only be measured in n-hexane (Fig. 8). In addition to the strong band at 3285 cm^{-1} a weaker one is found at 3372 cm^{-1}. Similar results have been reported for valinomycin in other solvents such as chloroform and carbon tetrachloride (23). The main IR absorption due to the carbonyl groups of valinomycin in n-hexane (Fig. 8) for example, is comparable to the absorption for the K^+ complex (Fig. 18). This similarity supports the existence of similar but not necessarily identical conformations. The rather narrow band of the NH stretching made in the typical range of hydrogen bonded NH frequencies as well as the remarkably narrow amide I band observed at comparably low frequency in n-hexane, indicate the presence of a conformation with strong intramolecular hydrogen bonds between the amide groups. The additional NH band of low intensity observed at a frequency characteristic for free NH and the inflection on the high frequency side of the amide I band (Fig. 8) are assigned to an additional conformational state of valinomycin in n-hexane where the intramolecular hydrogen bonds between the amide groups are partially broken. The interpretation of this IR study is consistent with earlier suggestions (23) that in nonpolar solvents such as n-hexane and carbon tetrachloride a closed structure with six intramolecular hydrogen bonds between the amide groups is predominantly formed (Fig. 9). According to the IR spectrum in n-hexane there is no direct evidence that a conformation characteristic of the crystalline state (24)

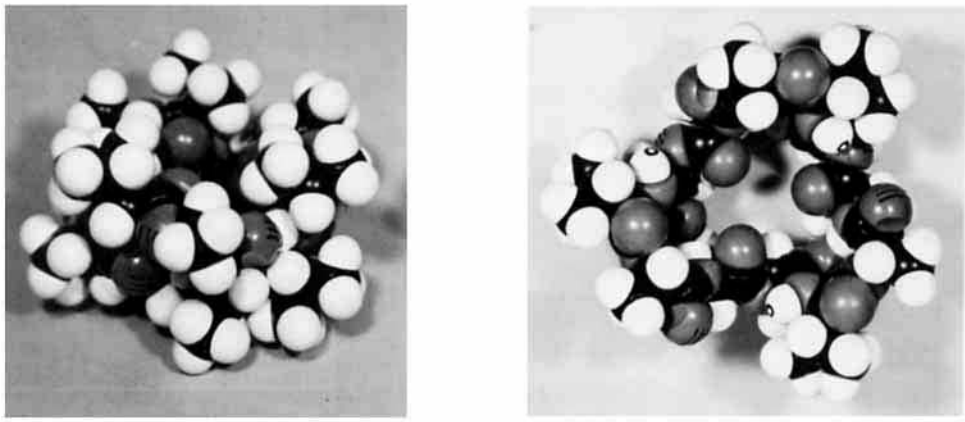

Fig. 9. Closed conformation of valinomycin (left) with six intramolecular hydrogen bonds and half-open conformation (right) with three intramolecular hydrogen bonds demonstrated with CPK molecular models.

exists in this solvent to any measureable extent. On the other hand, in more polar solvents such as dioxane, ethanol, and methanol, borad IR absorption bands of the ester and amide carbonyl groups are found (Fig. 18). These are expected for unfolded conformations of this molecule due to the intermolecular interaction of the carbonyl groups with solvent molecules. In addition, the position of the amide I band in methanol (Fig. 18) supports the existence of conformations characterized by a reduced number of intramolecular hydrogen bonds as compared to the case in n-hexane. No experimental evidence was found in these solvents to support the existence of the published conformation of the antibiotic in the crystalline state (24).

Additional details concerning the structural rearrangements in the solvent system n-hexane/ethanol (or d_{12}-cyclohexane/d_n-ethanol) can be derived from the ^{1}H–NMR spectra (Fig. 10). The NH and αCH signals of the same residues were identified by double resonance experiments. The assignment of signals for D- and L-valine residues was made according to (21). On this basis the signals of protons a, m, and x (cf. Fig. 10) are related to the D-valine fragments whereas those of protons A, M, and X are related to the L-valine fragments. A conformational change leading to the dissociation of intramolecular hydrogen bonds in a solvent system such as d_{12}-cyclohexane/d_n-ethanol is expected to be accompanied by an upfield shift of the NH signal. On the other hand, interaction of the free NH group with polar ethanol molecules should only cause a downfield shift of its NH signal due to intermolecular hydrogen bond formation. A reorientation of amide carbonyl groups induced by dissociation of intramolecular hydrogen bonds as well as of ester carbonyl groups of valinomycin is expected to influence the chemical shifts of corresponding αCH protons. However, a change of the magnetic anisotropy effect of the carbonyl group independent of differences in stereochemical relations can occur as a consequence of hydrogen bond formation with polar solvent molecules such as ethanol. Consequently, this effect can also lead to a change of the chemical shift of the neighboring αCH proton though it is expected that the latter effect contributes little to the chemical shift differences shown in Fig. 4 and Fig. 10. The observed dependence of the coupling constants on the solvent composition is mainly attributed to changes in dihedral angle of the structural elements. In order to dis-

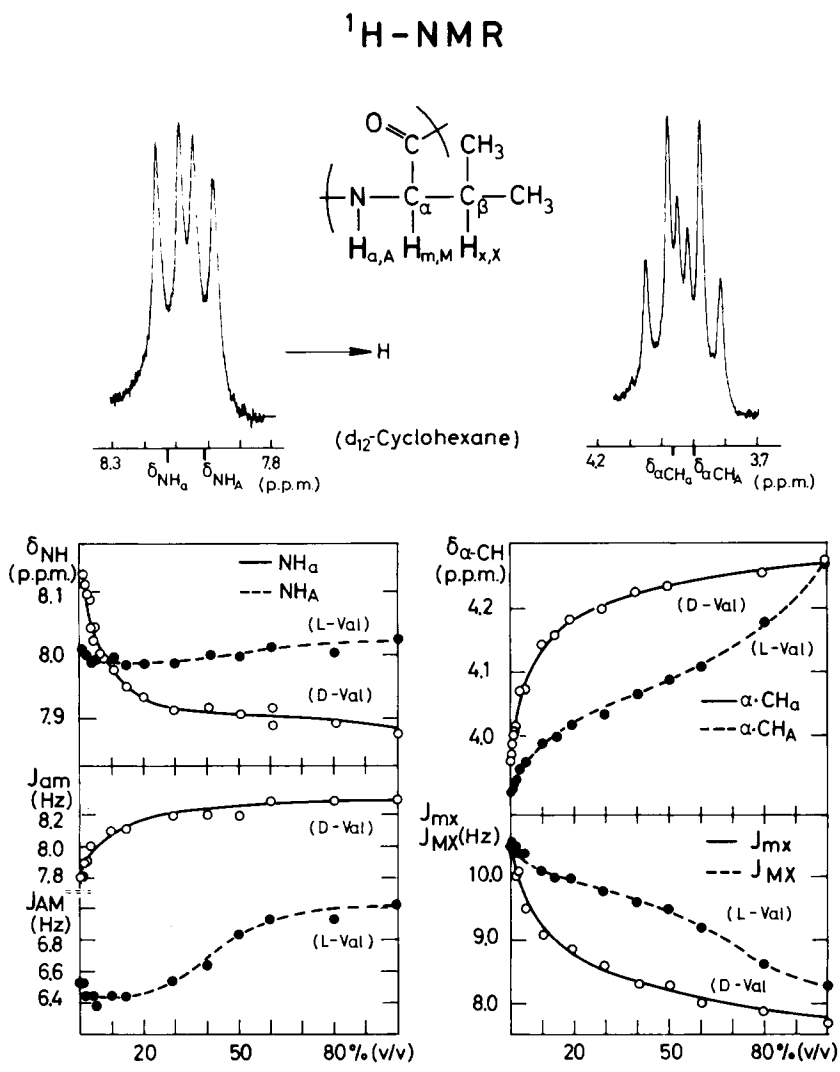

Fig. 10. Top: ^{1}H–NMR spectrum of NH and αCH protons due to valine residues of valinomycin in d_{12}-cyclohexane at 100 MHz. Bottom: The dependence of the chemical shifts (δ) and coupling constants (J) on solvent compostion [expressed as % d_n-ethanol in d_{12}-cyclohexane (v/v)] in the system d_{12}-cyclohexane/d_n-ethanol (n=5, 6). Details concerning the other symsbols used are discussed in the text.

cuss the experimental results on the basis of these effects it has further to be realized that D-valine and L-lactic acid and in contrast L-valine and D-α-hydroxy isovaleric acid residues are located in two different planes (Lac plane and Hyval plane) of the valinomycin molecule when a conformation stabilized by intramolecular hydrogen bonds is formed.

Between pure d_{12}-cyclohexane and 30% d_n-ethanol in d_{12}-cyclohexane only the signals of protons (H_a, H_m, H_x) of the D-valine residues showed significant changes (Fig. 10). The remarkable upfield shift of the NH_a signals (δ_{NH_a}) indicated that dissociation of intramolecular hydrogen bonds occurred predominantly in the Lac plane. Additional changes of other parameters ($\delta_{\alpha CH_m}$, $J_{NH_a\alpha CH_m}$, $J_{\alpha CH_m\beta CH_x}$) attributed to protons of D-valine fragments

only, e.g., changes of coupling constants indicating changes of the corresponding dihedral angles, were observed which exhibited the same dependence on solvent composition as was found for the shift of the NH_a signal. We conclude that those changes showing the same dependence on solvent composition are coupled together. Therefore, dissociation of intramolecular hydrogen bonds in the Lac plane is followed by an unfolding of those residues which are located in the same plane. The remarkably large value of the coupling constant $J_{\alpha CH_m \beta CH_x}$ suggests the presence of a rigid conformation with preferential trans orientation of the corresponding protons. An increase of the d_n-ethanol content was accompanied by a transition toward a less compact structure with predominant gauche orientation of the αCH and βCH protons which indicated an increase of rotational freedom for the sidechains of the D-valine residues.

The conformation of residues in the Hyval plane appeared to remain unchanged until the d_n-ethanol content exceeds about 30%. Further addition of d_n-ethanol induces a conformational change of those components located in the Hyval plane while no additional structural rearrangements were found under these conditions for those residues located in the Lac plane. Even in solutions of higher d_n-ethanol content (30% to 100% d_{12}-cyclohexane) the position of the NH_A signals remained unaffected, thus indicating that this conformational change cannot be induced by dissociation of intramolecular hydrogen bonds in the Hyval plane. Therefore it is concluded that this conformational rearrangement is predominantly caused by a reorientation of the ester groups in the Hyval plane. The latter reorientation is probably due to an interaction of ester carbonyl groups with ethanol molecules. These results indicate clearly that in the solvent system d_{12}-cyclohexane/d_n-ethanol at least three different conformational states are present. It is concluded that the previously suggested one-step conformational equilibrium (21) between a closed valinomycin conformation with six intramolecular hydrogen bonds and a half-open conformation with three intramolecular hydrogen bonds (Fig. 9) is too simple to explain these results.

According to the results obtained by ^{1}H--NMR the lifetimes of the individual conformational states are expected to be shorter than 10^{-2} to 10^{-3} sec. For a more detailed characterization of these various states relaxation techniques have been applied.

The ultrasonic absorption spectrum of valinomycin in n-hexane is characterized by a minimum of two relaxation processes around 10 MHz and 100 MHz (Fig. 11) with two corresponding relaxation times of 2×10^{-9} sec and 2×10^{-8} sec. Since the relaxation times are not sensitive to the valinomycin concentration these processes must be attributed to conformational rearrangements. Even in a solvent of pronounced nonpolar character such as n-hexane at least three predominant conformational states must be present (Table I). Small additions of ethanol distinctly change the ultrasonic absorption and cause a third relaxation process with a pronounced amplitude in the frequency range below I MHz (Fig. 11). This indicates the existence of a rather slow conformational transition. The frequency at the maximum amplitude could not be measured in n-hexane containing 17% ethanol. The corresponding relaxation time must be about 5×10^{-7} sec. Under the experimental conditions at least four main conformational states must be populated at equilibrium (cf. Table I). In solutions of higher ethanol content the low frequency relaxation process decreases (Fig. 11). Finally in pure methanol a nearly continuous ultrasonic absorption is observed (Fig. 20). This must be attributed to a spectrum of relaxation processes, for such an absorption profile would require description by at least four different relaxation times.

These ultransonic absorption studies of valinomycin are summarized in Table I, and clearly demonstrate the complexity of such a conformational analysis. The results also

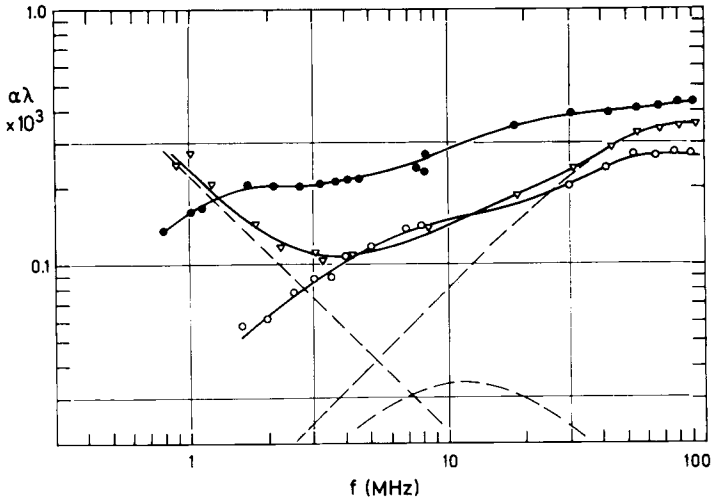

Fig. 11. Conformational transitions of valinomycin (10^{-2} M) in the solvent system n-hexane/ethanol. Frequency of ultrasonic excess absorption ($\alpha\lambda$) in n-hexane (○); 17% ethanol in n-hexane (v/v) (△); 50% ethanol in n-hexane (v/v) (●) T = 25°C). Analysis for single relaxation processes shown by dashed lines for the solvent 17% ethanol in n-hexane (v/v).

imply that a determination of all the predominant conformational states based on the available spectroscopic data is not possible at the present time. Summarizing, it is important to note that even in nonpolar solvents fast configurational rearrangements occur between conformers, and in more polar media a considerable number of conformations has to be considered. The rate constants of the slowest conformational transitions are of the order of magnitude of 10^7 sec^{-1}.

These conformational properties postulated on the basis of our spectroscopic and relaxation studies are in agreement with a model of conformational behavior for the valinomycin molecule shown schematically in Fig. 12. The closed form of the molecule (I), which is stabilized by six intramolecular hydrogen bonds, is opened stepwise with a reorientation of certain groups in solvents of increasing polarity to a conformational state with three hydrogen bonds (II). This structure is opened further by interaction with more polar solvent molecules such as methanol.

Gramicidin A. In nonpolar solvents gramicidin A is expected to exist as a dimer whereas in alcohols the monomer can also be detected at equilibrium (15, 25). According to these investigations conformational rearrangements occur which depend on solvent properties.

Ultrasonic absorption spectra of gramicidin A in the solvent system dibutyl ether/ethanol are shown in Fig. 13. In pure dibutyl ether no relaxation process can be detected. This indicates that a single predominant conformational state exists (18), most probably the dimer under our experimental conditions. This result would be consistent with the helical structures proposed for gramicidin A (15). On addition of ethanol the ultrasonic absorption increases remarkably and at least two relaxation processes can be detected in the frequency range 2 to 20 MHz (Fig. 13). Since the relaxation times are essentially independent of the

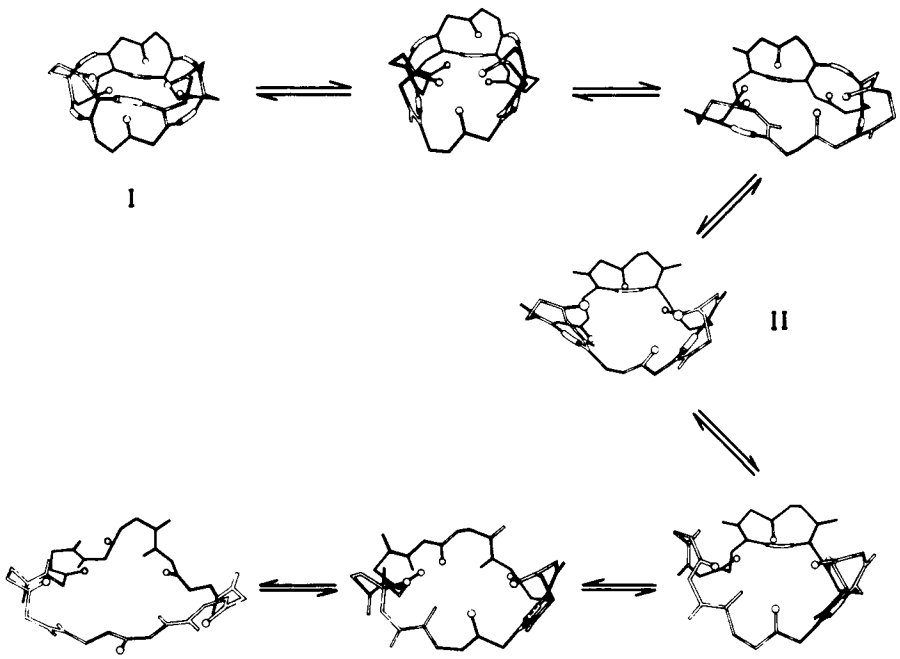

Fig. 12. Schematic diagram of conformational equilibria of valinomycin. Only the backbone of the molecule is shown with the oxygen atoms of the ester carbonyls (sidechains omitted). Intramolecular hydrogen bonds are drawn as connecting rods.

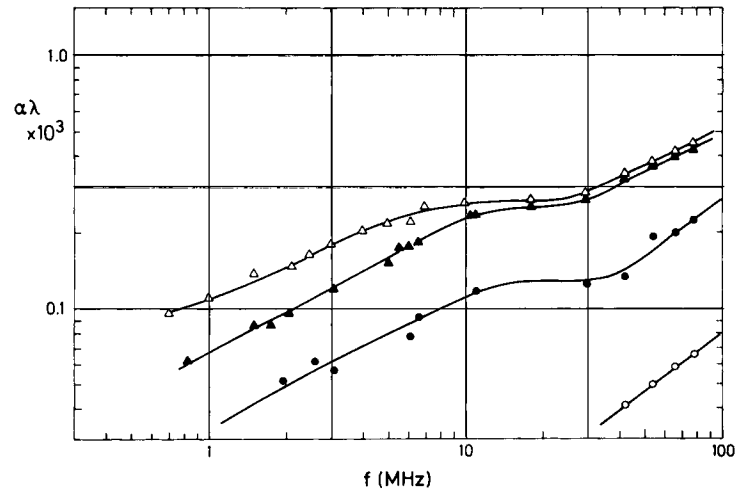

Fig. 13. Conformational transitions of gramicidin A in the solvent system dibutyl ether/ethanol. Frequency dependence of the ultrasonic excess absorption ($\alpha\lambda$) for 2×10^{-3} M gramicidin A in dibutyl ether (○); 5×10^{-3} M gramicidin A in 10% ethanol in dibutyl ether (v/v) (●); 7×10^{-3} M gramicidin A in 30% ethanol in dibutyl ether (v/v) (▲); 8×10^{-3} M gramicidin A in ethanol (△). (T = 25°C). The plotted absorption values are related to a normalized gramicidin A concentration of 8×10^{-3} M.

gramicidin A concentration, neither of these processes can be due to the direct dimerization reaction. They are therefore assigned to solvent induced conformational rearrangements of the monomer or dimer. As the amplitudes of these absorption processes are not linearly dependent on the gramicidin A concentration, a change in population between monomer and dimer is indicated.

The following simple kinetic reaction scheme would be consistent with the experimental results:

$$2\ G_1 \overset{\tau_1}{\rightleftharpoons} 2\ G_2 \overset{\tau_2}{\rightleftharpoons} G_2 - G_2 \overset{\tau_3}{\rightleftharpoons} G_3 - G_3$$

The two fast rearrangement steps characterized by the relaxation times τ_1 and τ_3 would contribute to the observed ultrasonic absorption processes. The dimerization step characterized by τ_2 is expected to be much slower. Additional evidence is of course required to exclude other mechanisms. In summary it is important to note that gramicidin A shows fast conformational rearrangements in solvents of intermediate polarity with rate constants around 10^7 sec^{-1} to 10^8 sec^{-1}. Similar rate constants are expected for the transport of cations through the gramicidin A channel in membranes.

Structure and Cation Specificity of Antibiotics

The outstanding property of membrane-bound antibiotics to differentiate between Na^+ and K^+ was related to specific complex formation with alkali ions. Crystals of antibiotic cation complexes (1:1) could be prepared which were suitable for X-ray diffraction analysis (26, 27). According to the crystal structure of the valinomycin K^+ complex (28) all six ester carbonyl groups are coordinated to the cation which is located in the central cavity of the ligand, as illustrated in Fig. 14. The conformation of the ligand in the complexed state is furthermore stabilized by the formation of six intramolecular hydrogen

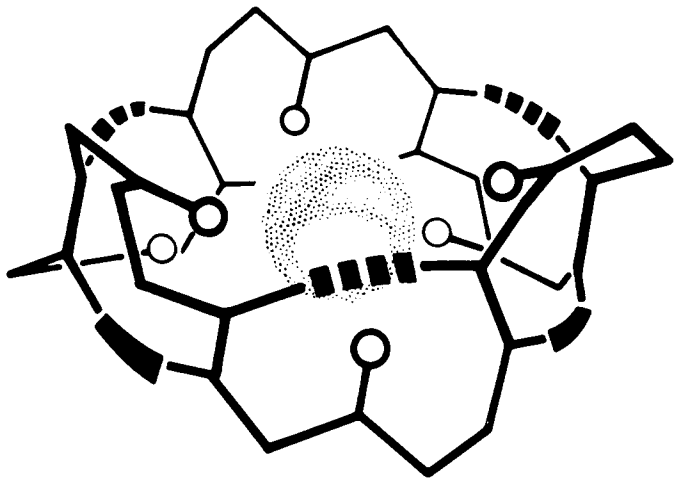

Fig. 14. Schematic illustration of the structure of the valinomycin K^+ complex. Only the backbone of the ligand is depicted with oxygen atoms of the ester carbonyl groups shown as open circles. The three intramolecular hydrogen bonds which are located in the upper plane are indicated by thick dotted lines and the three in the lower plane by thick solid lines.

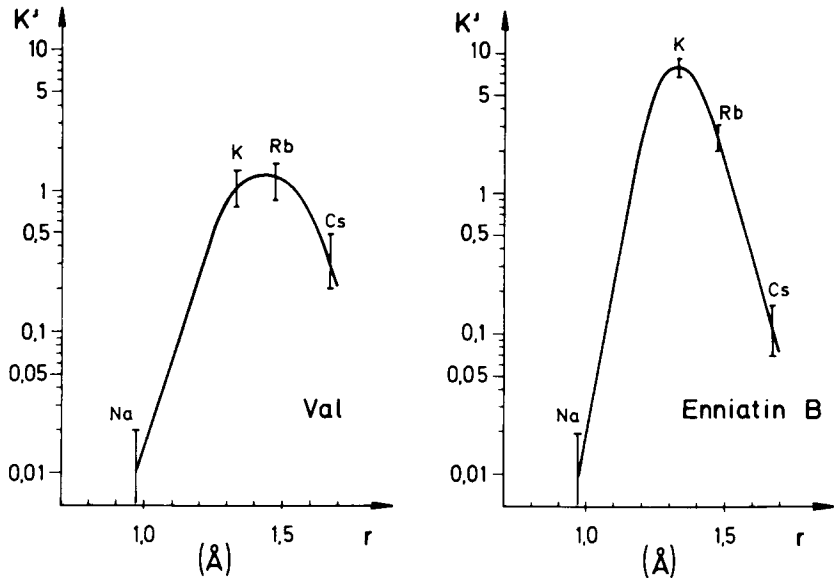

Fig. 15. Cation specificity of membrane-bound valinomycin and enniatin B. Apparent stability constants (K') of complexes of alkali ions as a function of the ionic radius. (Spectral titrations were carried out in a sonicated aqueous dispersion of 10^{-3} M to 5 x 10^{-3} M dimyristoyl L-lecithin; T = 25°C)

bonds between amide carbonyl and NH groups (Fig. 14). The antibiotic behaves similarly to a multidentate complexing agent.

Complex formation of membrane-bound antibiotics with cations occurs at the surface of phospholipid membranes. Spectral titrations of membrane-bound enniatin B and valinomycin with alkali ions employing UV- and CD-spectrometry were possible. The cation specificity of both membrane-bound cyclodepsipeptides is shown in Fig. 15, in which the apparent stability constants of the 1:1 complexes (activity coefficients neglected) are plotted as a function of the ionic radius. Valinomycin exhibits a distinct selectivity for potassium and rubidium. A similar selectivity is obtained for the membrane-bound enniatin B although the stabilities of its alkali ion complexes are much higher. Figure 16 shows the dependence of the stability constants for the 1:1 cation complexes of the same antibiotics with alkali ions in methanol as a function of ionic radius. In addition to this data, constants for NH_4^+, Tl^+, and Ag^+ complexes are also presented. The alkali ion specificity of valinomycin in methanol is similar to that of the membrane-bound valinomycin. A clear maximum is found for the stability of the Rb^+ complex. The values of the stability constants are much larger than those obtained in the phospholipid system. Among other reasons this may be due to the different dielectric constants. The data for the enniatin B alkali ion complexes in methanol indicate much lower specificity compared with the properties of the membrane-bound cyclodepsipeptide. The observed cation selectivities in methanol are consistent with the results of other studies (21, 29). Complex formation of gramicidin A with K^+ could not be detected in the polar solvents ethanol and methanol, indicating that gramicidin can only form very weak complexes. Our results clearly show that the essential molecular and mechanistic aspects of this cation specificity can be studied not only on the membrane-bound antibiotics but also in homogeneous solution.

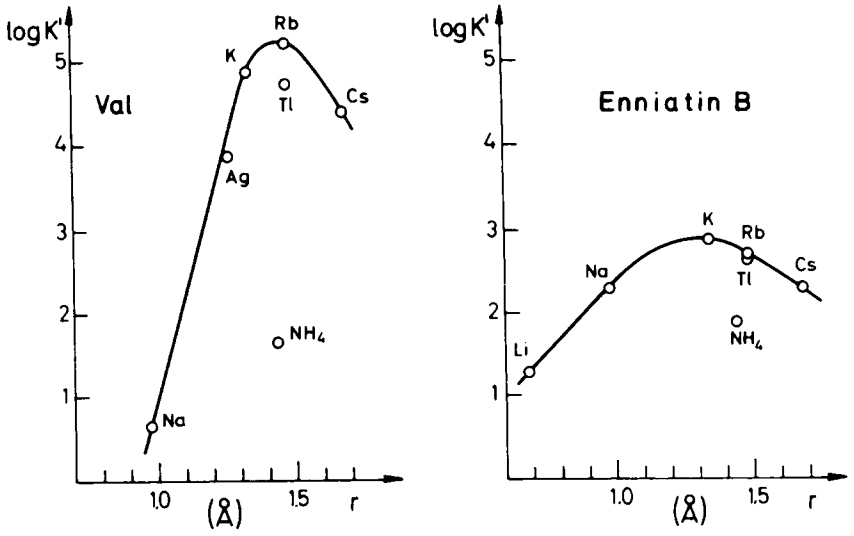

Fig. 16. Cation specificity of valinomycin and enniatin B in methanol. Apparent stability constants (K') of complexes of monovalent cations as a function of the ionic radius (T = 25°C)

The specific binding capability between two alkali ions is limited by the difference in their solvation energies. In order to reach a high specificity a complete replacement of the solvent molecules from the cations by the ligand is required. The maximum stability for a particular alkali ion is obtained when the difference between the free energies of hypothetical ligand binding in the absence of a solvent and the free energy of cation solvation passes through a maximum for the cation. This expected dependence of the ligand binding energy on the cation radius is essential for the cation specificity and is considered to be a consequence of the special conformational properties of the antibiotic (22, 30).

The remarkable difference in the stabilities of the valinomycin K^+ and Na^+ complexes can be correlated with the spectroscopic properties of these complexes. The CD spectra of the K^+, Rb^+, and Cs^+ complexes of valinomycin in methanol are characterized by a positive Cotton effect at about 210 mμ (Fig. 17). However, a negative Cotton effect is found for the Na^+ complex as shown in Fig. 17. This result indicates that the ligand conformation is considerably different depending on the nature of the bound cation. The ester carbonyl band of the IR spectrum of the valinomycin K^+ complex (Fig. 18) at 1745 cm^{-1} is symmetric and remarkably narrow compared to the corresponding band of the uncomplexed antibiotic in the same solvent where a considerable number of different conformational states are present. It is therefore concluded that the ester carbonyl groups of the K^+ complex exist in a single state in solution. The rather narrow and also symmetric amide I band at 1658 cm^{-1} of this group is consistent with an equivalent state of all the amide groups. The low frequency position of the amide I band is typical of those observed for strong intramolecular hydrogen bonds. The same interpretations are valid for the spectra of the Rb^+ and Cs^+ complexes. The IR absorption spectrum of the carbonyl stretching region of valinomycin in the presence of 1.7 M $NaClO_4$ (Fig. 18) reveals two broad bands due to the ester and amide carbonyl groups. The bandwidth observed indicates that no uniform state for all ester carbonyl groups exists in the Na^+ complex.

The dependence of the ^{13}C chemical shifts of valinomycin on the concentration of Na^+

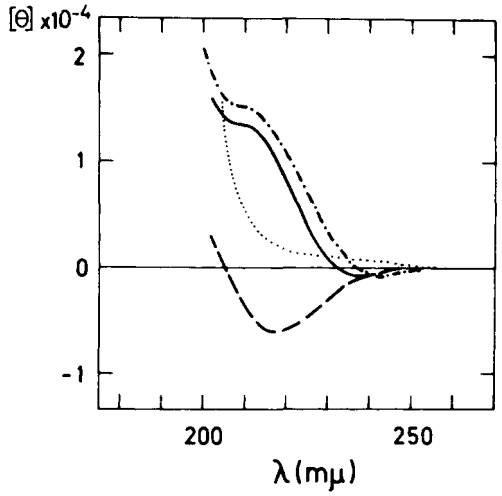

Fig. 17. Circular dichroism of valinomycin in methanol (· · · · ·) and in methanol containing 1.5 M $NaClO_4$ (– – –); 10^{-2} M KCl (——); 1.2×10^{-2} M CsCl (– · – · –). (T = 25°C)

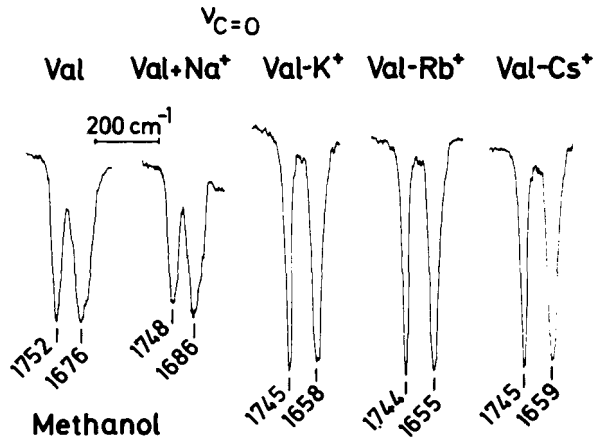

Fig. 18. Main bands of the IR absorption spectra of valinomycin and its alkali ion complexes [band positions are given in wave numbers (cm^{-1}), optical pathlengths were 0.1 mm unless otherwise specified]: 3.2×10^{-2} M valinomycin in methanol; 1.5×10^{-2} M valinomycin in methanol containing 1.7 M $NaClO_4$, pathlength 0.2 mm; 3.2×10^{-2} M valinomycin in methanol containing 6×10^{-2} M KCl; 3.2×10^{-2} M valinomycin in methanol containing 6.7×10^{-2} M CsCl.

and K^+ was measured in d_4-methanol (31) and is illustrated for the α-carbons in Fig. 19. Titration with KCl indicates that two of the four carbonyl signals are shifted much more strongly than the other two. In addition, the dependence of the chemical shift on the ratio [KCl]/[Val] is more pronounced for α-carbons of the amino acid than of both hydroxy acid residues. As a consequence of cation complexation the electron density of those carbons belonging to the coordinated ester carbonyl groups must decrease and a downfield shift of these signals is therefore expected. Thus the two low-field carbonyl signals in the spectrum of the K^+ complex as well as of the Rb^+ and Cs^+ complexes are assigned to the ester carbonyl carbons, which is consistent with earlier results (32, 33) obtained for the valinomycin K^+ complex. In contrast to the results obtained for the complexes of valino-

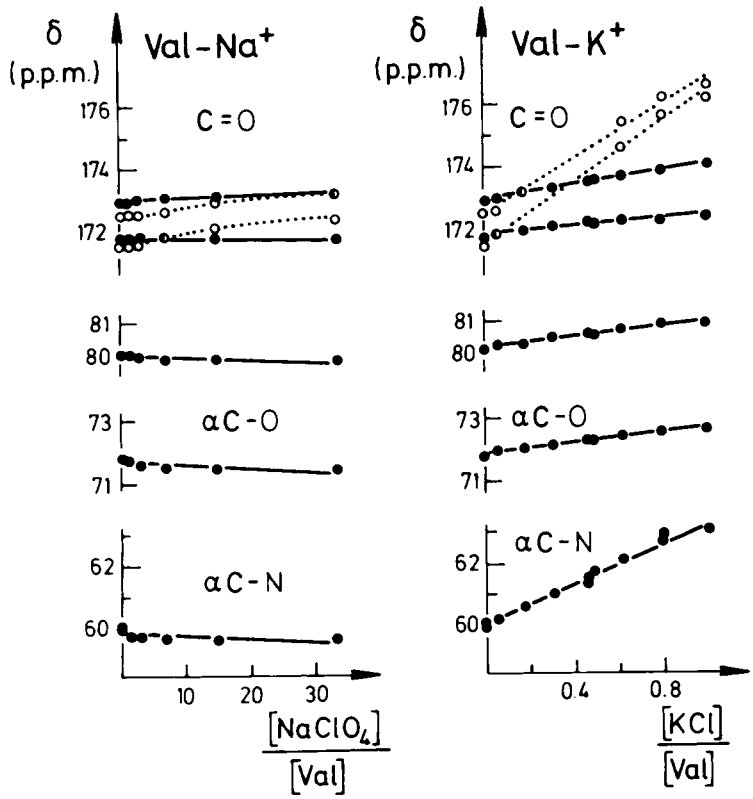

Fig. 19. Plot of the ^{13}C chemical shifts (δ) of carbonyl carbons and α-carbons of valinomycin dissolved in d_4-methanol against $[NaClO_4]$ / [Val] (left) and [KCl]/[Val] (right). (The open circles represent the ^{13}C chemical shifts of ester carbonyl carbons and are connected by broken lines.)

mycin with the large alkali ions K^+, Rb^+, and Cs^+, the shift differences observed upon complexation of Na^+ (Fig. 19) are much less pronounced. The ^{13}C–NMR spectrum of the Na^+ complex is considerably different and more closely resembles that of the uncomplexed antibiotic in polar solvents (31). This result leads also to the conclusion that in methanol the structure of the weak Na^+ complex must be considerably different from those of the larger alkali ions.

According to these IR absorption and ^{13}C–NMR investigations the ligand conformations of the K^+, Rb^+, and Cs^+ complexes in methanol are similar. They can be characterized by a coordination of the six ester carbonyl groups to the cations, thus leading to a rigid structure which is furthermore stabilized by the formation of six intramolecular hydrogen bonds between the amide groups. In contrast to these results the obviously different ligand conformation of the Na^+ complex in methanol is characterized by a reduced number of coordinated ester groups and intramolecular hydrogen bonds. Therefore the structure of this complex must be less compact and closed than those of the complexes with larger cations. As a consequence of the reduced number of coordinated ester carbonyl groups it may be possible that the bound Na^+ ion remains partially solvated. It is evident that the remarkable conformational differences of the ligand in the complexes with cations of different size contribute to the outstanding selectivity of this antibiotic.

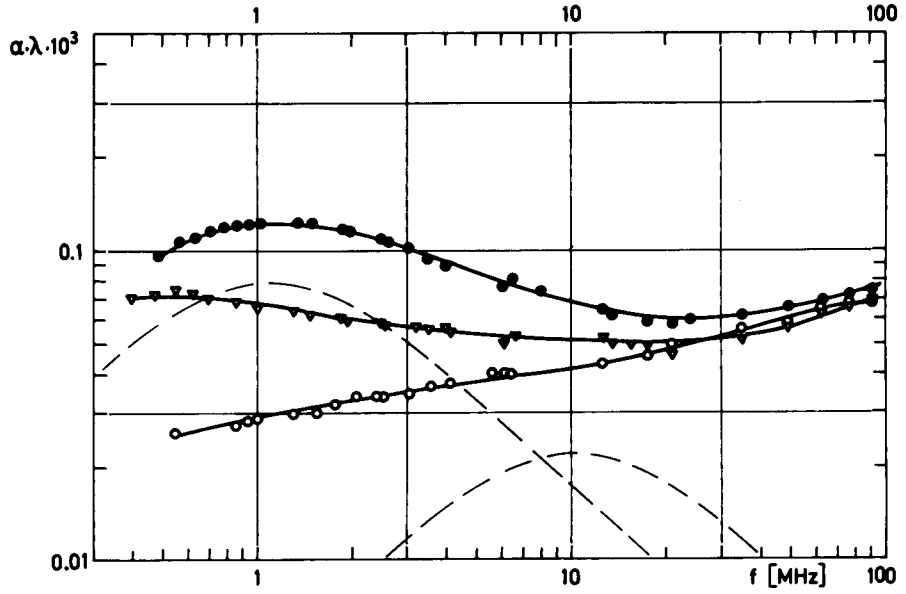

Fig. 20. Kinetics of complex formation of valinomycin with Na^+ ions in methanol. Frequency dependence of the ultrasonic excess absorption ($\alpha\lambda$) of 0.02 M valinomycin in methanol (○), 0.05 M $NaClO_4$ in methanol (△), 0.4 M $NaClO_4$ in methanol (●). (T = 25° C)

Dynamics and Cation Specificity of Antibiotics

A more detailed idea about the molecular mechanism of complex formation and cation selectivity can be derived from kinetic experiments. Recently kinetic measurements have been carried out which have contributed to the elucidation of the mechanism of specific ion complex formation in nonaqueous solvents (30, 34–37). In addition it has been suggested that a stepwise mechanism is involved in the solvent substitution of the cation by the ligand in order to account for the rather fast rate of complex formation of actins with alkali cations (22, 34, 35).

Since valinomycin exhibits the highest K^+/Na^+ selectivity of all the known ion specific antibiotics a detailed investigation of its mechanism of complex formation and alkali ion specificity is of interest in relation to the biological importance of these aspects in membrane processes. Therefore, relaxation experiments were carried out employing ultrasonic absorption and temperature-jump techniques. The complexation kinetics of the weak Na^+ and NH_4^+ complex could be studied only by ultrasonic absorption measurements (17, 22). At high $NaClO_4$ concentrations in methanol as the solvent, valinomycin shows an ultrasonic absorption spectrum having two relaxation processes around 1 MHz and 10 MHz (Fig. 20), respectively, which can be asigned to complex formation and are characterized by two relaxation times τ_1 and τ_2.

On the other hand the spectral changes observed in the UV upon complex formation (22) allowed kinetic studies on the more stable alkali cation complexes by temperature-jump relaxation spectrometry (19). Two relaxation processes have been observed for each of the K^+, Rb^+, and Cs^+ complexes in methanol containing 0.1 M tetra-n-butyl-ammonium perchlorate and they are attributed to the complexation reaction. A very fast relaxation

process ($\tau_1 < 5$ μsec), which cannot be resolved by this technique, is followed by a slower process with a relaxation time (τ_2) of the order of 200 μsec. The results of these kinetic investigations are consistent with the following simple kinetic reaction scheme, which is based on a two-step model for the complex formation:

$$V + \begin{matrix} \backslash \ /^{+} \\ Me \\ / \ \backslash \end{matrix} \underset{k_{21}}{\overset{k_{12}}{\rightleftharpoons}} \underset{\text{I}}{\lceil V - Me^{+} \rceil} \underset{k_{32}}{\overset{k_{23}}{\rightleftharpoons}} \underset{\text{II}}{\lceil V\text{–}Me^{+} \rceil}$$

In the first step a fast recombination between the solvated cation ($\begin{matrix} \backslash \ /^{+} \\ Me \\ / \ \backslash \end{matrix}$) and one of the opened conformations of valinomycin present in the polar medium leads to an intermediate complex (I). In the second step the formation of the stable cation complex (II) occurs by a first-order rearrangement.

This reaction scheme is characterized by two relaxation times. If the equilibration of the binding step is much faster than the subsequent reaction step ($k_{12} \gg k_{23}$, $k_{21} \gg k_{23}$) the dependence of the two relaxation times τ_1 and τ_2 on the free concentrations of the reaction partners (19) can be given as

$$1/\tau_1 = k_{21} + k_{12}\ (c_V + c_{Me}{}^{+}) \tag{11}$$

$$1/\tau_2 = k_{32} + \frac{k_{23}k_{12}\ (c_V + c_{Me}{}^{+})}{k_{21} + k_{12}\ (c_V + c_{Me}{}^{+})} \tag{12}$$

According to eq. (11), a linear concentration dependence is expected for $1/\tau_1$. The concentration dependence of $1/\tau_2$ according to eq. (12) is somewhat more complex and leads to a linear relationship for small free concentrations ($c_V + c_{Me}{}^{+}$), where $k_{21} \gg k_{12}(c_V + c_{Me}{}^{+})$

$$1/\tau_2 = k_{32} + \frac{k_{23}k_{12}\ (c_V + c_{Me}{}^{+})}{k_{21}} \tag{13}$$

At higher concentrations eq. (12) predicts saturation behavior: $1/\tau_2$ reaches a limiting value since $k_{12}\ (c_V + c_{Me}{}^{+}) \gg k_{21}$

$$1/\tau_2 = k_{32} + k_{23} \tag{14}$$

One of the relaxation times observed for complex formation with Na^+ and NH_4^+ ions follows eq. (11) as measured by ultrasonic absorption. However, the second relaxation time shows the more complex concentration dependence expected for τ_2 (12). This is shown in Fig. 21a for the Na^+ complex. The kinetic parameters for Na^+ and NH_4^+ complex formation are given in Table II.

Temperature-jump relaxation studies performed on the K^+, Rb^+, and Cs^+ complexes show a concentration dependent relaxation process in the 200 μsec range (17, 22). The latter relaxation times are characteristic of the linear, low concentration behavior of $1/\tau_2$ as given by eq. (13). The corresponding plot of $1/\tau_2$ as a function of ($c_V + c_K{}^{+}$) is shown in Fig. 21b.

The kinetics of complex formation can be discussed in terms of rate constants for the

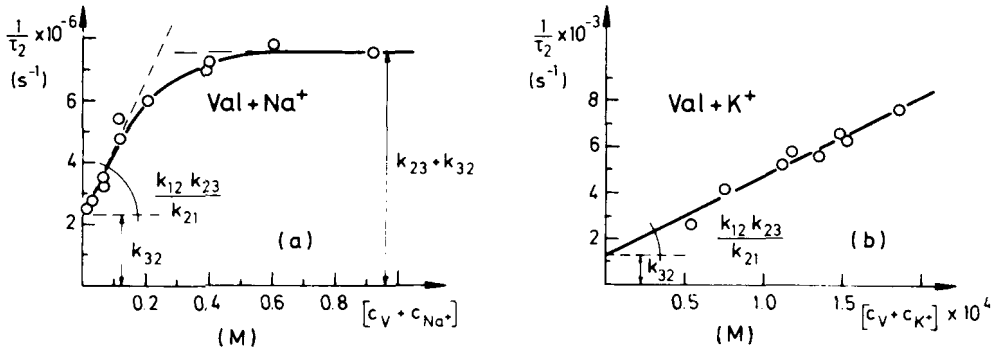

Fig. 21. Kinetics of the formation of the valinomycin Na^+ and K^+ (b) complexes in methanol: Concentration dependence of the inverse of the relaxation times $\frac{1}{\tau_2}$. (T = 25°C)

overall forward reaction k_{on} and reverse reaction k_{off}

$$k_{on} = \frac{k_{12}\ k_{23}}{k_{21} + k_{23}} \qquad (15) \qquad k_{off} = \frac{k_{21}\ k_{32}}{k_{21} + k_{23}} \qquad (16)$$

Under the reasonable assumption of a fast preequilibration process ($k_{21} \gg k_{23}$) eq. (15) and (16) simplify to (17) and (18), respectively,

$$k_{on} = \frac{k_{12}\ k_{23}}{k_{21}} \qquad (17) \qquad k_{off} = k_{32} \qquad (18)$$

These overall rate constants are directly measured for the K^+, Rb^+, and Cs^+ complexes and are given in Table II. Further details of the cation specificity of valinomycin can be discussed by comparing the kinetic parameters included in Table II.

The rate constants of the initial bimolecular reaction step for NH_4^+ complexation is slightly lower than the rate constant for a diffusion controlled ligand exchange reaction, whereas for Na^+ complexation k_{12} is substantially lower than diffusion controlled. However, they are both indicative of a rapid replacement of the inner solvation sphere around the cation as discussed for the formation of the monactin Na^+ complex (35). The initial reaction step already contributes to the specificity of the NH_4^+ complex as concluded from the higher K_{12} value of the NH_4^+ complex compared with the Na^+ complex. This may be due to the fact that the direct substitution mechanism is only involved in complex formation with metal ions. However, the stabilities of the Na^+ and K^+ precomplexes (I) with valinomycin are of the same order of magnitude (38). This indicates that the alkali ion specificity of the precomplexes (I) is rather poor. The main contribution to the specificity must therefore be due to the reaction steps which are involved in the conversion of the intermediate precomplex (I) to the final complex (II). Obviously these steps are very dependent on the conformational properties of the antibiotic.

The rate constants for the overall complex formation (k_{on}) for the K^+, Rb^+, and Cs^+ complexes are substantilly lower than the rate constants of diffusion controlled ligand exchange reactions (Table II). They are, however, in good agreement with the rate constants of the slowest conformational interconversions observed for the uncomplexed

Table II. Kinetic Parameters for the Formation of Valinomycin Cation Complexes in Methanol*

Cation	K′ (M^{-1})	k_{12} (M^{-1} sec^{-1})	k_{21} (sec^{-1})	$K_{12} = \frac{k_{12}}{k_{21}}$ (M^{-1})	k_{23} (sec^{-1})	k_{32} (sec^{-1})	$K_{23} = \frac{k_{23}}{k_{32}}$
NH_4^+	47	1×10^9	1.5×10^8	6.5	2×10^6	2.5×10^5	8
Na^+	4.7	7×10^7	2×10^7	3.5	4×10^6	2×10^6	2
K^+	3×10^4	k_{on} (M^{-1} sec^{-1}):	3.5×10^7			1.3×10^3	
Rb^+	6.5×10^4		5.5×10^7			7.5×10^2	
Cs^+	8×10^3		2×10^7			2.2×10^3	

*The kinetic parameters and the apparent stability constants (K′) of the K^+, Rb^+, and Cs^+ complexes have been measured in the presence of 0.1 M tetra-n-butylammonium perchlorate. The apparent stability constants (K′) were determined by spectrophotometric titrations. k_{on} and k_{off} are the overall reaction rate constants for forward and reverse reaction.

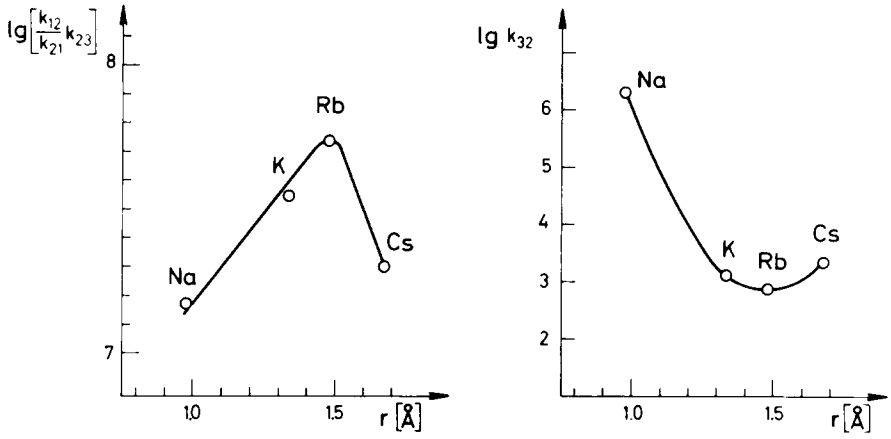

Fig. 22. Characteristic kinetic parameters for the formation ($[k_{12}/k_{21}]\ k_{23}$) and dissociation (k_{32}) of valinomycin alkali ion complexes as a function of the ionic radius.

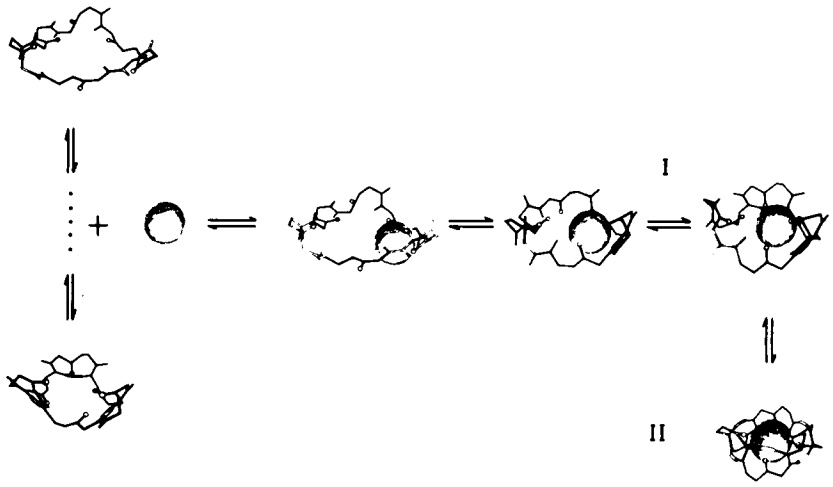

Fig. 23. Schematic diagram of the stepwise mechanism involved in complex formation of valinomycin with K^+. Only the backbone of the different ligand conformations is shown with the oxygen atoms of the ester carbonyl groups (side chains omitted). Intramolecular hydrogen bonds are drawn as connecting rods.

valinomycin in polar solvents. Consequently the rate determining step in the complexation reaction is taken to be the monomolecular structural change of the intermediate (I) due to a conformational rearrangement of the depsipeptide ligand after the initial binding of the cation has occurred.

The dependence of the overall rate constants k_{on} and k_{off} on the size of the cations is shown in Fig. 22. Both overall rate constants contribute to an optimal stability of the Rb^+ complex, since k_{on} reaches a maximum whereas k_{off} shows a minimum for this cation. Obviously valinomycin is adapted to cations of this size range not only in a thermodynamic sense but also with regard to the dynamic properties. The relative stabilities of complexes with cations of different size are largely the consequence of the varying rate constants of

complex dissociation as seen from the relative strong dependence of k_{off} on the ionic radius (Fig. 22). These dynamic characteristics are not only the result of differences in cation solvation energies. They must also be due to differences in the ligand conformations between the various cation complexes as indicated for example by the different spectroscopic properties of the Na^+ and K^+ complexes.

A molecular interpretation of the formal mechanism mentioned above in terms of plausible elementary steps is shown in Fig. 23. The recombination step between one of the opened conformations of valinomycin in methanol and the solvated K^+ ion can for example lead to the replacement of the first methanol molecule from the cation by one of the ester carbonyl groups of the antibiotic. Further stepwise solvent replacements are expected to occur until the intermediate complex (I) is reached. Although its structure has not been established, some of the possible intermediate states are indicated schematically in Fig. 23. The formation of the final complex (II) is initiated by the rate limiting conformational change of the ligand. This process is accompanied by a rapid replacement of the remaining solvent molecules until all six ester carbonyl groups are coordinated to the cation. A similar mechanism of action may obtain in the specific binding of alkali ions to their respective recognition sites in biological membrane systems.

CONCLUSIONS

Some conclusions can be reached which are based on the results of these kinetic investigations. In the case of the K^+ transport through phospholipid bilayer membranes mediated by valinomycin the rate constant of complex dissociation at the membrane surface is comparable to that of the cation transport through the interior of the membrane (12). In addition the stability of the membrane-bound valinomycin Na^+ complex is much lower than that of the corresponding K^+ complex (Fig. 15). It is therefore to be expected that the dissociation rate of the membrane-bound Na^+ complex would be much higher than the K^+ complex. This would be consistent with the kinetic data obtained in methanol (Table II). It can be assumed that the rate constants for the carrier transport of Na^+ and K^+ by valinomycin are of the same order of magnitude due to the fact that the diffusion process will be limited by the fluidity properties of the membrane. It must therefore be concluded that a preferential or specific transport of K^+ is observed since the rate of dissociation of the Na^+ complex is much faster than the rather slow rate of transport through the membrane.

With respect to gramicidin A we must assume that complex formation in methanol as well as of the membrane-bound antibiotic is very weak. Among other reasons the rather poor cation selectivity might be due to the fact that only a few solvent molecules can be substituted from the cation by this particular antibiotic. In this respect the properties of gramicidin A closely resemble those of the intermediate precomplexes of valinomycin which are also characterized by a small number of coordinated ester carbonyl groups and high dissociation rates (Table II). If it is assumed that the stability constants of gramicidin A cation complexes are smaller than 1 M^{-1} and that the formation rate constant is of the order of magnitude of 10^8 M^{-1} sec^{-1}, then the dissociation rate must be higher than 10^8 sec^{-1}. The latter value would be consistent with the dissociation rates (k_{21}) measured for the intermediate precomplexes of valinomycin with cations (Table II) as well as with the expected rate constant for cation transport through the gramicidin A channel.

ACKNOWLEDGMENTS

We are very grateful to Dr. R. O. Studer, F. Hoffmann-La Roche & Co., Basel, and to Dr. E. Gross, National Institutes of Health, Bethesda, Md., for making available to us the enniatin B and gramicidin A used in this work.

We wish to thank Dr. F. Eggers for his extensive collaboration in carrying out the ultrasonic absorption measurements.

We furthermore wish to thank Dr. H. -M. Schiebel, Gesellschaft für molekularbiologische Forschung, Stöckheim, and Dr. G. Englert, F. Hoffmann-La-Roche & Co., Basel, for their extensive cooperation in performing the ^{1}H–NMR studies on valinomycin and enniatin B. The authors are also very grateful to Profs., M. Eigen, G. Eisenman, D. W. Urry, J. McKinley McKee, Dr. R. S. Raylor, and Dr. D. A. Haydon for helpful and stimulating discussions.

REFERENCES

1. Plattner, P. A., Vogler, K., Studer, R. O., Quitt, P., and Keller-Schierlein, W., Helv. Chim. Acta 46:927 (1963).
2. Shemyakin, M. M., Ovchinnikov, Yu.A., Kiryushkin, A. A., and Ivanov, V. T., Tetrahedron Letters 885 (1963).
3. Shemyakin, M. M., Aldanova, N. A., Vinogradova, E. I., and Feigina, M. Yu., Tetrahedron Leters 1921 (1963).
4. Brockmann, H., Springorum, M., Träxler, G., and Höfer, I., Naturwiss. 50:689. (1963).
5. Sarges, R., and Witkop, B., J. Amer. Chem. Soc. 87:2011 (1965).
6. Moore, C., and Pressman, B. C., Biochem. Biophys. Res. Commun. 15:562 (1964).
7. Lardy, H. A., Graven, S. N., and Estrada -O. S., Fed. Proc. 26:1355 (1967).
8. Mueller, P., and Rudin, D. O., Biochem Biophys. Res. Commun. 26:398 (1967)
9. Tosteson, D. C., Andreoli, T. E., Tieffenberg, M., and Cook, P., J. Gen. Physiol. 51:373s (1968).
10. Eisenman, G., Cinai, S. M., and Szabo, G., Fed. Proc. 27:1289 (1968).
11. Krasne, S., Eisenman, G., and Szabo, G., Science 174:412 (1971).
12. Stark, G., Ketterer B., Benz, R., and Läuger, P., Biophys. J. 11:981 (1971).
13. Hladky, S. B., and Haydon, D. A., Nature 225:451 (1970); Biochim. Biophys. Acta 274:294 (1972).
14. Goodall, M. C., Arch. Biochem. Biophys. 147:129 (1971).
15. Urry, D. W., Goodall, M. C., Glickson, J. D., and Mayers, D. F., Proc. Nat. Acad. Sci. U. S. 68:1907 (1971).
16. Bamberg, E., and Läuger, P., J. Membrane Biol. 11:177 (1973).
17. Funck, Th., Eggers, F., and Grell, E., Chimia 26:637 (1972).
18. Grell, E., Eggers, F., and Funck, Th., Chimia 26:632 (1972).
19. Eigen, M., and De Maeyer, L., in "Techniques of Organic Chemistry", Vol. 8, Part 2, Interscience, New York, p. 895 (1963).
20. Eggers, F., and Funck, Th., Rev. Sci. Instr. (in press).
21. Shemyakin, M. M., Ovchinnikov, Yu.A., Ivanov, V. T., Antonov, V. K., Vinogradova, E. I., Shkrob, A. M., Malenkov, G. G., Evstratov, A. V., Laine, I. A., Melnik, E. I., and Ryabova, I. D., J. Membrane Biol. 1:402 (1969).
22. Grell, E., Funck, Th., and Eggers, F., in "Molecular Mechanisms of Antibiotic Action on Protein Biosynthesis and Membranes" E. Muñoz, F. García-Ferrándiz, and D. Vasques, (eds.), Elsevier, p. 646 (1972).
23. Ivanov, V. T., Laine, I. A., Abdulaev, N. D., Senyavina, L. B., Popov, E. M., Ovchinnikov, Yu. A., and Shemyakin, M. M., Biochem. Biophys. Res. Commun. 34:803 (1969).
24. Duax, W. L., Hauptman, H., Weeks, C. M., and Norton, D. A., Science 176:911 (1972).
25. Isbell, B. E., Rice-Evans, C., and Beaven, G. H., FEBS Lett. 25:192 (1972).
26. Kilbourn, B. T., Dunitz, J. D., Pioda, L. A. R., and Simon, W., J. Mol. Biol. 30:559 (1967).
27. Dobler, M., Dunitz, J. D., and Krajewski, J., J. Mol. Biol. 42:603 (1969).

28. Pinkerton, M., Steinrauf, L. K., and Dawkins, P., Biochem. Biophys. Res. Commun. 35:512 (1968).
29. Wipf, H. K., Pioda, L. A. R., Stefanac, Z., and Simon, W., Helv. Chim. Acta 51:377 (1968).
30. Funck, Th., Eggers, F., and Grell, E., in "Proceedings First European Biophysics Congress" E. Broda, A. Locker and H. Springer-Lederer, (Eds.), Verlag der Wiener Medizinischen Akademie, Wien, Vol. III, p. 37 (1971).
31. Grell, E., Funck, Th., and Sauter, H., Europ. J. Biochem. 34:415 (1973).
32. Bystrov, V. F., Ivanov, V. T., Koz'min, S. A., Mikhaleva, I. I., Khalilulina, K. Kh., Ovchinnikov, Yu.A., Fedin, E. I., and Petrovskii, P. V., FEBS Lett. 21:34 (1972).
33. Ohnishi, M., Fedarko, M.–C., Baldeschwieler, J. D., and Johnson, L. F., Biochem. Biophys. Res. Commun. 46:312 (1972).
34. Diebler, H., Eigen, M., Ilgenfritz, G., Maass, G., and Winkler, R., Pure Appl. Chem. 20:93 (1969).
35. Eigen, M., and Winkler, R., in "The Neurosciences" Second Study Program, F. O. Schmitt (Ed.), The Rockefeller University Press, New York, p. 685 (1970).
36. Haynes, D. H., Kowalsky, A., and Pressman, B. C., J. Biol. Chem. 25:502 (1969).
37. Haynes, D. H., FEBS Lett. 20:221 (1972).
38. Grell, E., Funck, Th., and Eggers, F., (in preparation).